Research Article

Journal of PeptideScience

Received: 10 June 2011 Revised: 18 July 2011 Accepted: 3 August 2011 Published online in Wiley Online Library: 3 November 2011

(wileyonlinelibrary.com) DOI 10.1002/psc.1414

The structure and assembly model of the third transmembrane domain of Slc11a1 in SDS micelles revealed by NMR study of the Leu-substituted peptide

Shuyan Xiao, Lei Yang and Fei Li*

Slc11a1 is an integral membrane protein with 12 putative transmembrane domains (TMDs) and functions as a pH-coupled divalent metal cation transporter. The conservation of three negatively charged residues in the TMD3 of Slc11 protein family implies the important role of this domain in the function of the proteins. However, aggregation of the transmembrane peptide in micelles prevents structural study of the peptide in these membrane-mimetic environments by NMR spectroscopy. Here, we characterized the structure, position, and assembly model of Slc11a1-TMD3 (Lys128-Ile151) in SDS micelles by the NMR study of its Leu-substituted peptide. It was found that the two-site substitutions of Ala for Leu residues at positions 136 and 140 of TMD3 disrupt the aggregation without altering the secondary structure of the peptide. The Leu-substituted peptide folds as an α-helix spanning from Leu133 to Gly144 and embedded in the micelles. A Leu zipper is suggested to account for the self-assembly of the wild-type peptide in SDS micelles. Copyright © 2011 European Peptide Society and John Wiley & Sons, Ltd.

Supporting information can be found in the online version of this article.

Keywords: Slc11a1-TMD3; structure; assembly; topology

Introduction

Slc11a1 (solute carrier family 11a member 1; formerly known as Nramp1, natural-resistance-associated macrophage protein 1) belongs to a protein family that highly conserved from bacteria to human. Slc11a1 is a pH-dependent divalent cation transporter expressed primarily in late endosomal/lysosomal compartment of macrophages and polymorphonuclear leukocytes [1–3]. The predicted amino acid sequence of Slc11a1 identifies a highly hydrophobic integral membrane glycoprotein composed of 12 predicted transmembrane domains (TMDs), several putative phosphorylation sites in predicted intracellular loops, a glycosylated site in extracytoplasmic loop 7/8, and a 'transport motif' in the cytoplasmic loop 8/9. Both *N*-terminus and *C*-terminus are predicted to be cytoplasmic [4,5]. In mouse, the innate resistance or susceptibility to infection with intracellular parasites such as *Mycobacteria*, *Salmonella*, and *Leishmania* is controlled by Slc11a1 [6,7]. In human, Slc11a1 is involved in susceptibility to autoimmune and infectious diseases, such as rheumatoid arthritis, juvenile rheumatoid arthritis, diabetes, Crohn's disease, sarcoidosis, tuberculosis, and leprosy [8–14].

Although Slc11a1 was discovered first, but because of limitations of its expression, much of what we know about Slc11a1 is derived in part from parallel studies of other Slc11 homologs. As another member of Slc11 family, Slc11a2 is ubiquitously expressed in most tissues and cell types and extensively studied. Predicted amino acid sequence analysis of the Slc11 molecule indicates that Slc11a1 and Slc11a2 sequences share 64% identity in the coding region of the mRNAs [15]. The absolute conservation of three charged residues in TMD3 of Slc11 sequences suggests an important role of this TMD for the functions of Slc11 proteins [16]. The acidic residue Glu154 in TMD3 of Slc11a2 appears to be essential for transport function because the E154A mutation results in a complete loss of function [17]. Similar results have been also obtained from mutagenesis studies in MntH (Slc11 homolog in *E. coli*). The mutation of Glu102 (corresponding to Glu154 in Slc11a2) to Gln or Asp was found to cause complete loss of function. The mutageneses of residues Asp109 and Glu112, also placed in TMD3 of MntH, resulted in partial loss of transport function [18,19]. In addition, Czachorowski *et al.* [20] obtained the structural models of Slc11 using the LeuT crystal structure as a template. The model suggested that the most conserved elements of the Slc11 hydrophobic core, TMD1, 3, 6, and 8, play key roles in the cation-driven membrane transport mechanism [20,21]. Hence, determination of the structure of TMD3 in membrane-mimetic environments should help us to better understand the mechanism of divalent metal-ion transport by Slc11 proteins and the role of TMD3 in transport.

In the beginning of this study, we tried to use SDS and DPC detergents as membrane mimics to determine the three-dimensional structure of the TMD3 peptide. Unfortunately, the qualities of the NMR spectra of the peptide in the micelles were rather poor and prevented structural determination. As a result, we previously

* *Correspondence to: Fei Li, State Key Laboratory of Supramolecular Structure and Materials, Jilin University, 2699 Qianjin Avenue, Changchun 130012, China. E-mail: feili@jlu.edu.cn*

State Key Laboratory of Supramolecular Structure and Materials, Jilin University, Changchun 130012, China

investigated the structure of Slc11a1 TMD3 in 60% HFIP-d_2 aqueous solution [22]. Although this study provided some insights into the structure of the peptide, it has been reported that detergent provides a better environment than the organic solvent for structure determination. Furthermore, the topology of the peptide in membrane could also be detected in detergent environment. In this study, we demonstrated that poor NMR spectra of the peptide in SDS micelles arose from its strong propensity for self-association in the micelles. We tried to explore the crucial residues for assembly and to obtain the structure and topology of the peptide in SDS micelles through mutations that can disrupt the aggregation but maintain the secondary structure of the peptide. By analyzing the sequence of the peptide, we found that the first 15 residues of TMD3 comprise seven Leu or Ile residues. Previous study has shown that abundant Leu or Ile residues running along one side of an amphipathic alpha helix may serve as protein–protein interaction domains and induce protein self-association by the so-called 'Leu zipper', and the substitution(s) of one Leu residue or two at 'a' and/or 'd' positions with Ala in the Leu zipper motif may impair the self-association [23]. Therefore, we envisioned that the assembly of TMD3 may arise from the Leu zipper motif, and two Leu residues at positions 136 and 140 of TMD3 peptide might be involved in the zipper motif. As a result, the two Leu residues were substituted by Ala simultaneously. This mutation would be expected to have minimum disruptive effect on the α-helical structure but disrupt the self-association of the peptide [24–27]. As expected, the spectra of the peptide were remarkably improved, and NMR assignment could be made unambiguously.

Materials and Methods

Materials

The peptide 128-Lys-Val-Pro-Arg-Ile-Leu-Leu-Trp-Leu-Thr-Ile-Glu-Leu-Ala-Ile-Val-Gly- Ser-Asp-Met-Gln-Glu-Val-Ile-151, corresponding to the TMD3 of Slc11a1 128–151, and its mutant with two-site Ala substitutions in positions 136 and 140 were used in this study. For the sake of simplicity, the amino acid sequence of TMD3 segment was numbered according to the peptide (beginning from 1) but not the protein (beginning from 128) in the following sections. The peptides were synthesized by Biopeptide Company and GL Biochem Ltd. One lysine residue was added to the *C*-terminus of the mutant peptide to increase the solubility. The purity of both peptides was confirmed by analytical HPLC and MS to be >95%. The deuterated reagents SDS-d_{25} (98%) and D_2O (99.8%) were purchased from Cambridge Isotope Laboratories (Andover, MA, USA). The solvent HFIP (99.5%) was purchased from Acros Organics (Morris Plains, NJ, USA). All chemicals were used as purchased directly without further purification.

Sample Preparation

The peptide previously dissolved in 0.36 ml HFIP was added into 0.2 ml SDS-d_{25} aqueous solution. The mixture was diluted by addition of 5.56 ml H_2O. The solution was lyophilized overnight to remove the solvent completely. The resulting powder was dissolved in 0.6 ml aqueous solution with 90% H_2O and 10% D_2O to obtain an NMR sample of 2 mM peptide in 240 mM SDS-d_{25}. The pH value of the sample was adjusted by addition of a small amount of NaOH or HCl solution directly using a micro pH electrode (Hamilton, Reno, NV, USA). For the paramagnetic probe experiments, the 16-DSA dissolved in methanol-d_4 or $MnCl_2$ dissolved in H_2O was added into the SDS-d_{25} micellar solution of the peptide to obtain a final concentration of 4 mM for the spin label or 0.02 mM for Mn^{2+} ions.

The samples of the peptide in SDS micelles with various molar ratios of peptide to SDS for the fluorescence measurements were prepared similarly. The concentration of SDS was fixed to 10 mM, whereas the concentration of peptide was varied in the range of [peptide] : [SDS] from 1 : 1000 to 1 : 100. The pH values of the samples are approximately 6.

Fluorescence Spectroscopy

Tryptophan fluorescence experiments were performed on RF-5301PC fluorescence spectrophotometer at room temperature. The fluorescence spectra were collected in the range of 290–420 nm using excitation of 280 nm, excitation slit of 3 nm, emission slit of 3 nm, sampling interval of 0.2 nm, and medium scan rate. Three spectra were recorded and averaged, and the reference spectrum of the respective medium was subtracted.

NMR Experiments

NMR experiments were carried out at 298 K on a Bruker Avance 500-MHz spectrometer (Fällanden, Switzerland) equipped with a 5-mm triple resonance inverse probe with *z*-gradient coil. Two-dimensional NOESY experiments were recorded with mixing time of 200 ms, transients of 48–128. Two-dimensional TOCSY experiments were acquired using the MLEV-17 pulse sequence [28] performed with mixing time of 50, 75, and 100 ms, transients of 48–96. All the spectra were collected with 2048 data points in F2 dimension and 512 data points in F1 dimension. Water suppression was achieved by WATERGATE (water suppression by gradient tailored excitation) technique. The proton chemical shifts were referenced to TSP [sodium salt of 3-(trimethylsilyl)-propionate-2,2,3,3-d_4]. The spectra were processed with XWINNMR software (version 3.5, Bruker, Fällanden, Switzerland), and NMR assignments were obtained using SPARKY software [29].

Structure Calculation

The tertiary structures of the peptides were calculated using the program CYANA (version 1.0.6) [30]. Calculations started from 200 initial random structures, 20 structures with the lowest target function values, which have no distance constraint violations greater than 0.2 Å and no dihedral angle constraint violations greater than 5° were selected and then further energy minimized with the AMBER7 force field [31]. The stereochemical qualities of the peptide structure were evaluated by PROCHECK-NMR software [32]. Three-dimensional structures were displayed with MOLMOL software [33].

Results and Discussion

Structure and Assembly

The ^{1}H-NMR spectra of the wild-type TMD3 peptide in SDS-d_{25} micelles were very poor at various pH values, though the dispersion of the spectra became better at alkalescent pH values than at acidic pH values. Very weak intensities and severe overlapping of the signals in the 2D ^{1}H-NMR spectra prevented a complete signal assignment, particularly assignment of the cross-peaks between residues, and determination of three-dimensional structure of the peptide. Nevertheless, most of the Hα and HN resonances

Journal of PeptideScience

and some side-chain resonances of the wild-type peptide at different pH values were still assigned with combination of TOCSY and NOESY spectra. More than one set of resonances from the *C*-terminal residues Ser18-Ile24 in the 2D NMR spectra of the wild-type peptide were indentified at neutral or higher pH values (it is not clear at lower pH values because of much poorer spectra) (Figure 1). These heterogeneous spin systems display close Hα chemical shifts but evidently different HN chemical shifts. This suggests that the wild-type peptide may be self-assembled with similar monomeric structure in SDS micelles. Whereas most of the region of the peptide is homogeneously surrounded (characterized by the same HN resonances) for the monomers in an assembly, the *C*-terminal segments may be exposed to different environments (characterized by different HN resonances) possibly because of different interactions of the *C*-terminal segments with SDS micellar surface. Some of the *C*-terminal segments may be located beneath SDS surface (state A in Figure 1), and some may be more exposed to water (states B and C in Figure 1).

Leucine zippers are a special class of heptad repeats, which contain Leu or Ile at *a*-position and *d*-position of an amphipathic alpha helix with Leu or Ile residues running along one side. The hydrophobic interactions between Leu/Ile residues provide a driving force for aggregation [26]. The substitution of amino acids at *a*-position and *d*-position can alter the assembly of the protein. TMD3 is a Leu/Ile abundant peptide segment with Leu9 and Leu13 just occupying *a*-position and *d*-position if they are involved in a helix. We hypothesized that the poor spectra of the peptide result from assembly driven by Leu zipper. Accordingly, we replaced two Leu residues at positions 9 and 13 of the peptide with Ala. As expected, the NMR spectra of the mutant peptide were dramatically improved, the heterogeneous resonances disappeared, and the assignments of the resonances were unambiguously obtained (Figure 2). The remarkable improvement of NMR spectra is attributed to the dissociation of the peptide assembly induced by the substitution.

To obtain the direct evidence of the wild-type peptide aggregation in SDS micelles, we recorded the fluorescence spectra of the wild-type and L9A/L13A-substituted peptides at various [peptide]/[SDS] molar ratios. In comparison with the fluorescence spectra of the mutant peptide with emission maximum of 332 nm, the spectra of the wild-type peptide display an increase in the intensity and a blue shift of emission maximum (314 nm), suggesting that the tryptophan of the wild-type peptide is located in a less polar environment than that of the mutant. The fluorescence intensities at the emission maxima were plotted for the two peptides as a function of [peptide]/[SDS] molar ratio (Figure 3). Whereas the fluorescence intensity of tryptophan in the mutant peptide increases linearly

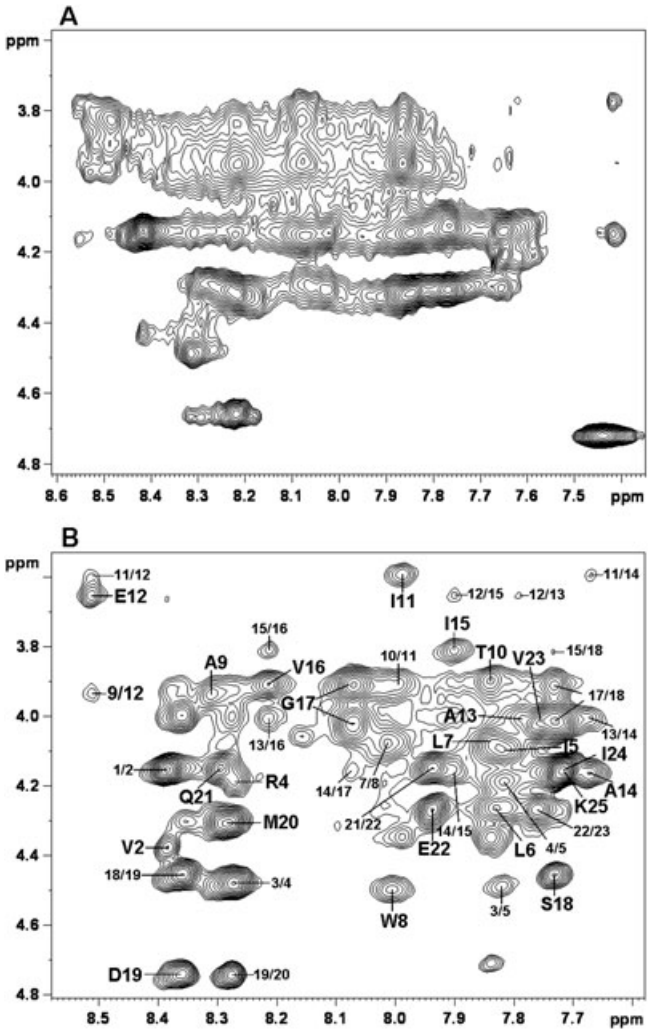

Figure 2. Hα-HN region of 2D NOESY spectra for the wild-type peptide (A) and Leu-substituted peptide (B) at pH 5.5.

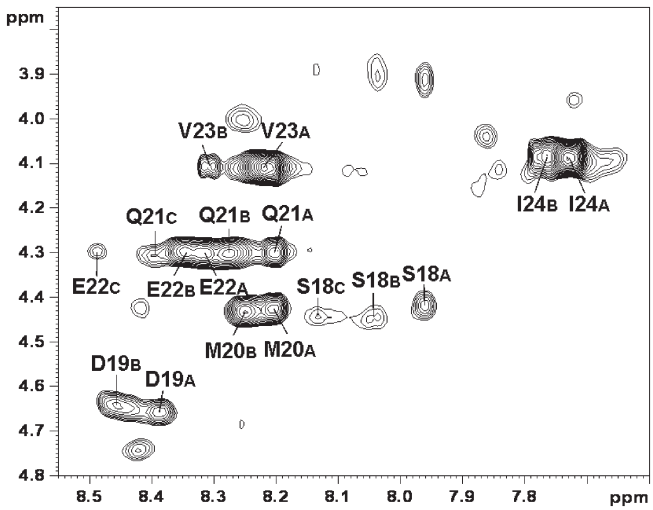

Figure 1. Hα-HN region of the TOCSY spectrum for the wild-type peptide at pH 6.5.

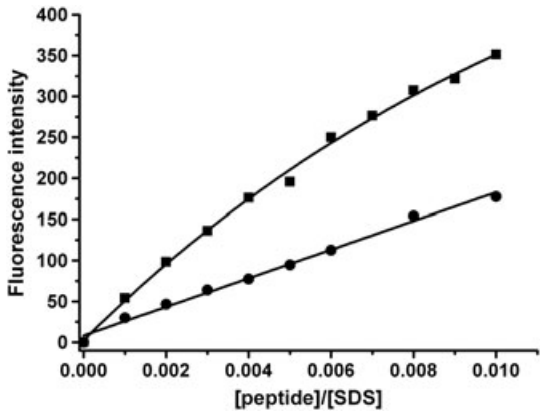

Figure 3. Fluorescence intensity of the wild-type peptide (■) and Leu-substituted peptide (●) with increasing [peptide]/[SDS] molar ratio.

with [peptide]/[SDS] ratio, the fluorescence intensity of tryptophan in the wild-type peptide is partially quenched with increasing [peptide]/[SDS] ratio. This indicates that the wild-type peptide is self-associated [34]. The approaching of indole rings between tryptophan residues in an aggregate leads to quenching of tryptophan fluorescence. The extent of fluorescence quenching depends on the fraction of the peptide in the aggregate state and the distance between tryptophan residues.

The secondary structure shifts $\Delta\delta_{ss}$ of both peptides define an α-helix structure in the same residue region (Figure 4), indicating that the substitutions of Leu with Ala do not change the secondary structure of the TMD segment. Therefore, we can obtain the structure information of the wild-type peptide by determining the structure of the Leu-substituted peptide. In the NOESY spectra of the Leu-substituted peptide incorporated with SDS micelles, a series of short-range NOE connectivities (H$\alpha(i)$–HN$(i+1)$ and HN(i)–HN$(i+1)$) and numerous medium-range connectivities (H$\alpha(i)$–HN$(i+3)$, H$\alpha(i)$–HN$(i+4)$, and H$\alpha(i)$–H$\beta(i+3)$) were observed, suggesting the existence of an α-helix (Figure 5). A total of 243 nonredundant distance constraints resulting from 442 NOE cross-peaks in the NOESY spectrum at pH 5.5 were used in the structure calculation, and an α-helix ranging from Leu6 to Gly17 with flexible *C*-terminal part was obtained (Figure 6). The residues Leu6, Ala9, Ala13, and Val16 are located at the same side of the helix. Further analysis of the structures with PROCHECK-NMR showed that all the residues involved in the helical span fall in the allowed region of Ramachandran plot (90% of the residues lie within the most favored region and 10% within additionally allowed region).

The secondary structure shift data indicated that both the wild-type and Leu-substituted peptides form helix in the same residue region. Therefore, the structure of the wild-type peptide in SDS micelles should be assumed as an α-helix spanning over Leu6-Gly17 with the residues Leu6, Leu9, Leu13, and Val16 at the same side of the helix. These residues, or at least the three Leu residues, may be involved in the assembly by Leu zipper. We supposed that the wild-type peptide assembles as a trimer on the basis of the observation of three groups of cross-peaks in the TOCSY spectra of the peptide at higher pH values. A model of helical bundle of the peptide was illustrated by the helical wheel projection (Figure 7). In this trimeric model, the Leu6, Leu9, Leu13, and Val16 face the inside of the bundle and form a Leu zipper by the hydrophobic interactions between monomers, and the negatively charged residues Glu12 and Asp19 are located at the side of the hydrophobic core.

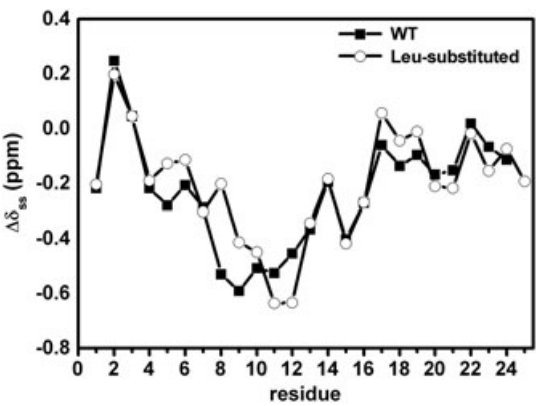

Figure 4. Secondary structure shift $\Delta\delta_{ss}$ of the wild-type and Leu-substituted peptides at pH 5.5.

Figure 5. NOE connectivities of the Leu-substituted peptide at pH 5.5.

Previously, we determined the structure of the TMD3 peptide in 60% HFIP-d_2 aqueous solution [22] and found that the peptide forms a helix spanning over Ile5-Met20. In this study, we obtained a helix structure spanning over Leu6-Gly17 for the TMD3 peptide in SDS micelles, nearly a helical-turn shorter in the *C*-terminal part than the structure of the peptide in 60% HFIP-d_2 aqueous solution. This may arise from the interactions of the Asp19 and Glu22 with the micellar head groups (Topology Determined by Paramagnetic Probe section) that hindered the formation of helical turn in the *C*-terminus.

pK_a of Ionizable Residues

The pK_a values of ionizable residues provide useful information about the electrostatic environment of these residues and thus interactions between a given ionizable residue and its surrounding groups. Each ionizable residue has its own standard pK_a value in model tetrapeptides [35]. If a pK_a value is away from standard, the perturbations result may be from hydrogen bond interactions, charge–charge interactions, or solvent inaccessibility [36,37]. NMR is a powerful method for measurement of pK_a values of ionizable residues through pH-dependent chemical shifts.

Because of the limitation of spectral quality, only some of pH titration data from the state A of the wild-type peptide in SDS-d_{25} micelles were obtained. The pK_a values were obtained by the analysis of the titration curves using modified Hill equation [38].

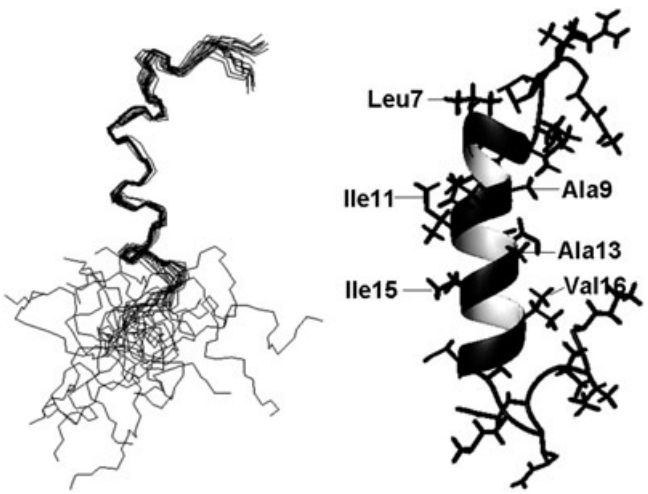

Figure 6. Ensemble of 20 structures with the lowest target functions and the ribbon representation of the Leu-substituted peptide at pH 5.5.

Journal of PeptideScience

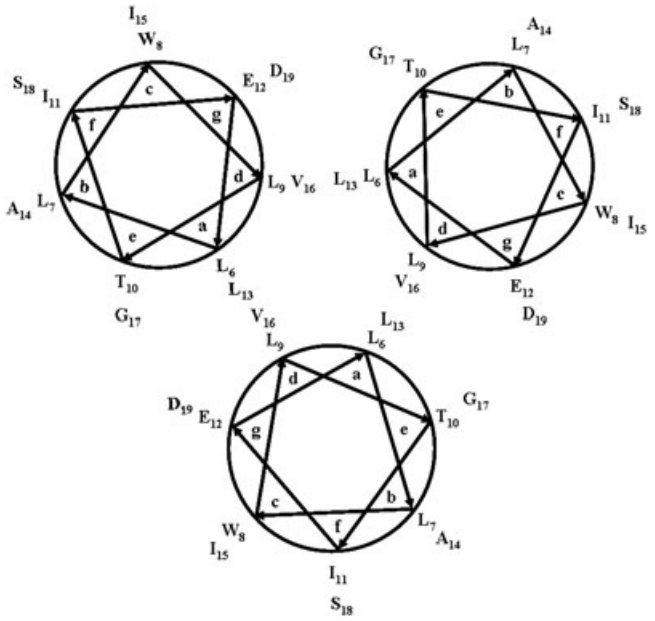

Figure 7. The helical wheel projection, which shows the peptide trimer mediated by the Leu zipper.

Because the resonances of Glu12 could not be unambiguously identified at lower pH, the titration curves of Glu12 were not obtained. However, the pK_a value of Glu12 can be estimated by the midpoint of the pH curve, pH_m, of the residues in the vicinity of Glu12. The pH dependence of the resonances of surrounding groups arises from the interactions with the carboxyl group of ionizable residue either through bonds or through space. The pK_a or pH_m values from identifiable resonances with $|\Delta\delta| > 0.2$ ppm are listed in Table 1. The pH_m values from the neighboring residues of Glu12 are approximately 6.4–6.8, whereas the pK_a values of Asp19 (Hβ) and Glu22 (Hγ) are 5.6 and 5.4, respectively; all of them are higher than the pK_a values of Asp (3.9) and Glu (4.3) in model peptides [35], indicating that the three negatively charged residues in the wild-type peptide are located at the inside of SDS micelles. The residue Glu12 may be buried in the interior of the micelles, and the residues Asp19 and Glu22 may be near the head groups of the micelles.

We also measured the pK_a values of the Leu-substituted peptide. The pK_a values of Glu12 (Hγ), Asp19 (Hβ), and Glu22 (Hγ) are 5.9, 5.1, and 5.3, respectively; all of them are higher than the pK_a values in model peptides but lower than those of the wild-type peptide. This indicates that the mutant peptide is also inserted in SDS micelles, but these residues are surrounded by more polar environments. The side chains of Glu12 and Asp19 in the mutant peptide extend to the head-group region of the micelles. The assembly of the wild-type peptide in SDS micelles restricts the movement of Glu12 to the surface of the micelles, resulting in larger pK_a values. The substitution of Leu with Ala disturbed the assembly of the peptide, allowing the movement of Glu12 to the head-group region of SDS micelles.

Table 1. The pH titration parameters for some titratable residues of the wild-type peptide with $|\Delta\delta| > 0.2$ ppm

Proton	pK_a/pH_m	$\Delta\delta$ (ppm)	Proton	pK_a/pH_m	$\Delta\delta$ (ppm)
Leu9-HN	6.83 ± 0.07	−0.452	Ser18-HN	6.81 ± 0.04	0.257
Thr10-Hα	6.73 ± 0.09	0.265	Asp19-HN	6.06 ± 0.04	0.258
Ile11-Hα	6.64 ± 0.02	0.268	Asp19-Hβ	5.58 ± 0.02	−0.274
Leu13-Hα	6.54 ± 0.07	0.286	Gln21-Hα	5.39 ± 0.05	0.230
Leu13-HN	6.39 ± 0.08	−0.496	Glu22-HN	5.50 ± 0.09	0.631
Ala14-HN	6.79 ± 0.07	0.464	Glu22-Hγ	5.42 ± 0.08	−0.268
Val16-HN	5.99 ± 0.05	−0.366	Val23-HN	5.55 ± 0.01	0.483

Topology Determined by Paramagnetic Probe

The position of the mutant peptide with respect to the surface or the interior of the micelles was investigated by paramagnetic probe experiments using 16-DSA and Mn^{2+}, which affect the relaxation rate of nuclei close to them and make the NMR signals broadened. The free radical of 16-DSA is localized near the micellar core, so it induces broadening of resonances of the nuclei near the center of the micelle [39], whereas Mn^{2+} ions induce broadening of the peaks of amino acid residues that are solvent exposed or close to aqueous environment [40]. The paramagnetic probe experiments of the wild-type peptide were not performed because of the poorly resolved 2D ^{1}H-NMR spectra of the wild-type peptide. The paramagnetic broadening effects of the probes on the NMR signals of the mutant peptide were indicated by the intensity ratio of each Hα-HN cross-peak in 2D NOESY spectra acquired after and before addition of the probes (Figure 8).

Basically, the resonance intensities of the *N*-terminal residues Val2, Arg4, and Ile5 of the mutant peptide are totally quenched by 16-DSA, whereas the intensities of other residues are less or moderately affected. In contrast, the resonance intensities of the *C*-terminal residues Asp19-Lys25, especially Asp19, Glu22, Ile24, and Lys25, are dramatically affected by Mn^{2+} ions, whereas those from other residues are less affected. This suggests that the position of the peptide in the micelles is between the head

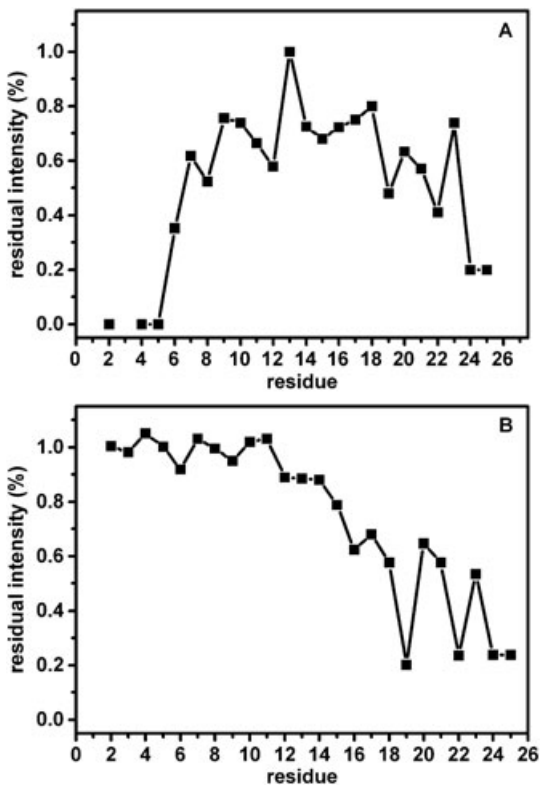

Figure 8. The effects of 16-DSA (A) and Mn^{2+} (B) on the resonance intensities of the Leu-substituted peptide at pH 5.5.

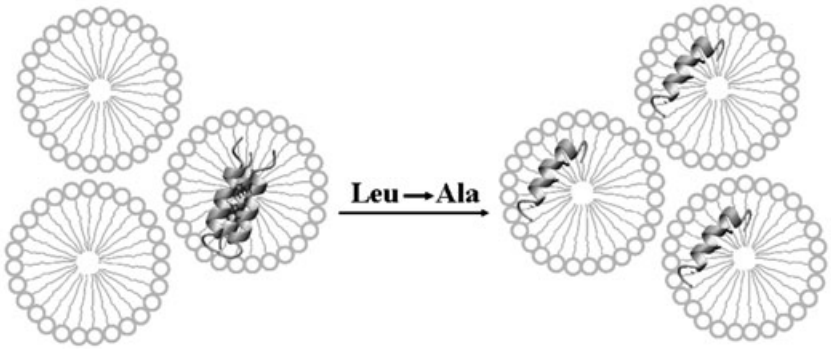

Figure 9. The scheme for the dissociation process of the TMD3 peptide resulting from the two-site Leu substitutions.

groups and the center of the hydrophobic kernel with the *N*-terminal residues near the core of the micelles and the *C*-terminal residues, especially the charged residues, close to the surface of the micelles. This is in agreement with the results of pK_a. On the basis of the pK_a data and the paramagnetic probe results, we proposed the topological models for the wild-type peptide at the associate and dissociate states (Figure 9). The structure of the peptide in the associate state is stabilized mainly by the hydrophobic interactions between peptide and SDS micellar core, whereas the structure in dissociate state is stabilized by both the polar interactions of the residues Glu12 and Asp19 with the head groups of SDS micelles and apolar interactions of the hydrophobic side of the peptide with SDS hydrophobic core. In the context of the full protein, the topology of the peptide obtained in SDS micelles likely means an oblique orientation of TMD3 in biological membranes. TMD3 may be engaged in interhelical contacts by oblique arrangement during transport [20].

Summary

The NMR study reveals that TMD3 segment of Slc11a1 has a strong propensity to aggregate to form an α-helix bundle in the micelle state by Leu-zipper interaction. The residues Leu9/Leu13 in the TMD3 peptide may play a crucial role for the self-association of the peptide. The simultaneous substitutions of L9A/L13A cause dissociation of the peptide assembly while maintaining its α-helical structure. The tertiary structure of the TMD3 wild-type peptide can be well represented by the structure of the Leu-substituted peptide. The peptide might be embedded in the membrane at a shallow position because of the extension of Glu12 toward the head-group region of the membrane if the aggregate is prohibited.

Acknowledgements

This work was supported by grants from the National Natural Science Foundation of China (NSFC 20973083 and 20934002).

References

1 Wardrop SL, Wells C, Ravasi T, Hume DA, Richardson DR. Induction of Nramp2 in activated mouse macrophages is dissociated from regulation of the Nramp1, classical inflammatory genes, and genes involved in iron metabolism. *J. Leukoc. Biol.* 2002; **71**: 99–106.
2 Vidal S, Malo D, Vogan K, Skamene E, Gros P. Natural resistance to infection with intracellular parasites: isolation of a candidate for *Bcg*. *Cell* 1993; **73**: 469–485.
3 Govoni G, Gauthier S, Billia F, Iscove NN, Gros P. Cellspecific and inducible Nramp1 gene expression in mouse macrophages in vitro and in vivo. *J. Leukoc. Biol.* 1997; **62**: 277-286.
4 Gruenheid S, Pinner E, Desjardins M, Gros P. Natural resistance to infection with intracellular pathogens: the *Nramp1* protein is recruited to the membrane of the phagosome. *J. Exp. Med.* 1997; **185**: 717–730.
5 Govoni G, Gros P. Macrophage NRAMP1 and its role in resistance to microbial infections. *Inflamm. Res.* 1998; **47**: 277–284.
6 Skamene E, Schurr E, Gros P. Infection genomics: Nramp1 as a major determinant of natural resistance to intracellular infections. *Annu. Rev. Med.* 1998; **49**: 275–287.
7 Vidal SM, Pinner E, Lepage P, Gauthier S, Gros P. Natural resistance to intracellular infections: *Nramp1* encodes a membrane phosphoglycoprotein absent in macrophages from susceptible (*Nramp*1D169) mouse strains. *J. Immunol.* 1996; **157**: 3559–3568.
8 Ates Ö, Müsellim B, Öngen G, Topal-Sarıkaya A. NRAMP1 (SLC11A1): a plausible candidate gene for systemic sclerosis (SSc) with interstitial lung involvement. *J. Clin. Immunol.* 2008; **28**: 73–77.
9 Shaw D, Clayton SE, Atkinson H, Williams N, Miller D, Blackwell JM. Linkage of rheumatoid arthritis to the candidate gene NRAMP1 on 2q35. *J. Med. Genet.* 1996; **33**: 672–677.
10 Nishino M, Ikegami H, Fujisawa T, Kawaguchi Y, Kawabata Y, Shintani M, Ono M, Ogihara T. Functional polymorphism in Z-DNA-forming motif of promoter of SLC11A1 gene and type 1 diabetes in Japanese subjects: association study and meta-analysis. *Metabolism* 2005; **54**: 628–633.
11 Hofmeister A, Neibergs HL, Pokorny RM, Galanduik S. The natural resistance-associated macrophage protein gene is associated with Crohn's disease. *Surgery* 1997; **122**: 173–179.
12 Maliarik MJ, Mei CK, Sheffer RG, Rybicki BA, Major ML, Popovich J, Iannuzzi MC. The natural resistance associated macrophage protein gene in African Americans with sarcoidosis. *Am. J. Respir. Cell Mol. Biol.* 2000; **22**: 672–675.
13 Bellamy R, Ruwende C, Corrah T, McAdam KP, Whittle HC, Hill AV. Variations in the NRAMP1 gene and susceptibility to tuberculosis in West Africans. *N. Engl. J. Med.* 1998; **338**: 640–644.
14 Abel L, Sanchez FO, Oberti J, Thuc NV, Hoa LV, Lap VD, Skamene E, Lagrange PH, Schurr E. Susceptibility to leprosy is linked to the human NRAMP1 gene. *J. Infect. Dis.* 1998; **177**: 133–145.
15 Gruenheid S, Cellier M, Vidal S, Gros P. Identification and characterization of a second mouse *Nrarnp* gene. *Genomics* 1995; **25**: 514–525.
16 Cellier M, Privé G, Belouchi A, Kwan T, Rodrigues V, Chia W, Gros P. Nramp defines a family of membrane proteins. *Proc. Natl. Acad. Sci. U.S.A.* 1995; **92**: 10089–10093.
17 Lam-Yuk-Tseung S, Govoni G, Forbes J, Gros P. Iron transport by Nramp2/DMT1: pH regulation of transport by 2 histidines in transmembrane domain 6. *Blood* 2003; **101**: 3699–3707.
18 Courville P, Chaloupka R, Cellier MF. Recent progress in structure function analyses of Nramp proton-dependent metal-ion transporters. *Biochem. Cell Biol.* 2006; **84**: 960–978.
19 Haemig HA, Brooker RJ. Importance of conserved acidic residues in MntH, the Nramp homolog of *Escherichia coli*. *J. Membr. Biol.* 2004; **201**: 97–107.
20 Czachorowski M, Lam-Yuk-Tseung S, Cellier M, Gros P. Transmembrane topology of the mammalian Slc11a2 iron transporter. *Biochemistry* 2009; **48**: 8422–8434.
21 Courville P, Urbankova E, Rensing C, Chaloupka R, Quick M, Cellier MF. Solute carrier 11 cation symport requires distinct residues in transmembrane helices 1 and 6. *J. Biol. Chem.* 2008; **283**: 9651–9658.

22 S Xiao, Y Wang, L Yang, H Qi, C Wang, F Li, Study on structure and assembly of the third transmembrane domain of Slc11a1, *J. Pept. Sci.* 2010; **16**: 249–255.
23 Ahmad A, Yadav SP, Asthana N, Mitra K, Srivastava SP, Ghosh JK. Utilization of an amphipathic leucine zipper sequence to design antibacterial peptides with simultaneous modulation of toxic activity against human red blood cells. *J. Biol. Chem.* 2006; **281**: 22029–22038.
24 Heinz DW, Baase WA, Matthews BW. Folding and function of a T4 lysozyme containing 10 consecutive alanines illustrate the redundancy of information in an amino acid sequence. *Proc. Natl. Acad. Sci. U.S.A.* 1992; **89**: 3751–3755.
25 O'Neil KT, DeGrado WF. A thermodynamic scale for the helix-forming tendencies of the commonly occurring amino acids. *Science* 1990; **250**: 646–651.
26 O'Shea EK, Rutkowski R, Kim PS. Evidence that the leucine zipper is a coiled coil. *Science* 1989; **243**: 538–542.
27 Luo Z, Matthews AM, Weiss SR. Amino acid substitutions within the leucine zipper domain of the murine coronavirus spike protein cause defects in oligomerization and the ability to induce cell-to-cell fusion. *J. Virol.* 1999; **73**: 8152–8159.
28 Bax A, Davis DG. MLEV-17-based two-dimensional homonuclear magnetization transfer spectroscopy. *J. Magn. Reson.* 1985; **65**: 355–360.
29 Goddard TD, Kneller DG. SPARKY 3, University of California, San Francisco.
30 Güntert P, Mumenthaler C, Wüthrich K. Torsion angle dynamics for NMR structure calculation with the new program DYANA. *J. Mol. Biol.* 1997; **273**: 283–298.
31 Pearlman DA, Case DA, Caldwell JW, Ross WS, Cheatham III TE, DeBolt S, Ferguson D, Seibel G, Kollman P. AMBER, a package of computer programs for applying molecular mechanics, normal mode analysis, molecular dynamics and free energy calculations to simulate the structural and energetic properties of molecules. *Comp. Phys. Commun.* 1995; **91**: 1–41.
32 Laskowski RA, Rullmann JA, MacArthur MW, Kaptein R, Thornton JM. AQUA and PROCHECK-NMR: programs for checking the quality of protein structures solved by NMR. *J. Biomol. NMR* 1996; **8**: 477–486.
33 Koradi R, Billeter M, Wüthrich K. MOLMOL: a program for display and analysis of macromolecular structures. *J. Mol. Graph.* 1996; **14**: 51–55.
34 Kelkar DA, Chattopadhyay A. Modulation of gramicidin channel conformation and organization by hydrophobic mismatch in saturated phosphatidylcholine bilayers. *Biochim. Biophys. Acta* 2007; **1768**: 1103–1113.
35 Bundi A, Wüthrich K. ^{1}H-NMR parameters of the common amino acid residues measured in aqueous solutions of the linear tetrapeptides H-Gly-Gly-*X*-L-Ala-OH. *Biopolymers* 1979; **18**: 285–297.
36 Song J, Laskowski M Jr, Qasim MA, Markley JL. NMR determination of pKa values for Asp, Glu, His, and Lys mutants at each variable contiguous enzyme inhibitor contact position of the turkey ovomucoid third domain. *Biochemistry* 2003; **42**: 2847–2856.
37 Laurents DV, Huyghues-Despointes BM, Bruix M, Thurlkill RL, Schell D, Newsom S, Grimsley GR, Shaw KL, Treviño S, Rico M, Briggs JM, Antosiewicz JM, Scholtz JM, Pace CN. Charge-charge interactions are key determinants of the pK values of ionizable groups in ribonuclease Sa (pI=3.5) and a basic variant (pI=10.2). *J. Mol. Biol.* 2003; **325**: 1077–1092.
38 Xiao S, Li J, Wang Y, Wang C, Xue R, Wang S, Li F. Identification of an "α-helix-extended segment-α-helix" conformation of the sixth transmembrane domain in Slc11a2. *Biochim. Biophys. Acta* 2010; **1798**: 1556–1564.
39 Van Den Hooven HW, Spronk CA, Van De Kamp M, Konings RN, Hilbers CW, Van De Ven FJ. Surface location and orientation of the lantibiotic nisin bound to membrane-mimicking micelles of dodecylphosphocholine and of sodium dodecylsulphate. *Eur. J. Biochem.* 1996; **235**: 394–403.
40 Lindberg M, Gräslund A. The position of the cell penetrating peptide penetratin in SDS micelles determined by NMR. *FEBS Lett.* 2001; **497**: 39–44.

